# Journal Pre-proof

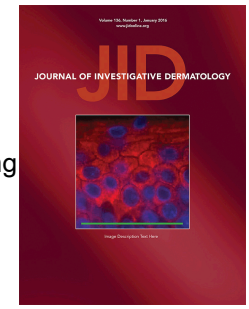


Dermal Fibroblast CCN1 Expression in Mice Recapitulates Human Skin Dermal Aging

Taihao Quan, Yaping Xiang, Yingchun Liu, Zhaoping Qin, Yan Yang, George Bou-Gharios, John J. Voorhees, Andrzej A. Dlugosz, Gary J. Fisher

PII: S0022-202X(20)31967-9

DOI: https://doi.org/10.1016/j.jid.2020.07.019

Reference: JID 2582

To appear in: *The Journal of Investigative Dermatology*

Received Date: 17 January 2020

Revised Date: 6 July 2020

Accepted Date: 7 July 2020

Please cite this article as: Quan T, Xiang Y, Liu Y, Qin Z, Yang Y, Bou-Gharios G, Voorhees JJ, Dlugosz AA, Fisher GJ, Dermal Fibroblast CCN1 Expression in Mice Recapitulates Human Skin Dermal Aging, *The Journal of Investigative Dermatology* (2020), doi: https://doi.org/10.1016/j.jid.2020.07.019.

# Dermal Fibroblast CCN1 Expression in Mice Recapitulates Human Skin Dermal Aging

Taihao Quan[1], Yaping Xiang[1], Yingchun Liu[1], Zhaoping Qin[1], Yan Yang, George Bou-Gharios[2], John J Voorhees[1], Andrzej A. Dlugosz[1], Gary J Fisher[1]

[1]Department of Dermatology, University of Michigan Medical School, Ann Arbor, Michigan USA

[2]Institute of Ageing and Chronic Diseases, University of Liverpool, Liverpool UK

ORCIDs: Taihao Quan, 0000-0002-0954-5109; Yaping Xiang, 0000-0002-5591-8690; Yingchun Liu, 0000-0003-2392-9114; Zhaoping Qin, 0000-0003-2439-5417; Yan Yang, 0000-0002-9739-1807; George Bou-Gharios, 0000-0002-9563-9418; John J Voorhees, 0000-0003-1856-785X; Andrzej A. Dlugosz, 0000-0002-9791-3257; Gary Fisher 0000-0002-6065-6242.

To whom correspondence should be addressed:

Taihao Quan, thquan@med.umich.edu

1150 W. Medical Center Drive

Medical Science I, Room 6447

Ann Arbor, Michigan 48109 USA

Telephone: (734) 615-2403

Short Title: Dermal skin aging model

Abbreviations used: Extracellular matrix (ECM), type I collagen alpha chain 2 (COL1A2), CCN family member 1 (CCN1), Transforming growth factor-beta (TGF-β), Activator protein 1 (AP-1), Matrix Metalloproteinase (MMP), Atomic Force Microscopy (AFM), Type I/II TGF-β

receptor (TβRI/TβRII), Heparin Sulfate Proteoglycans (HSPG), Ultraviolet (UV), Reactive Oxygen Species (ROS).

**ABSTRACT**

The aging process deleteriously alters the structure and function of dermal collagen. These alterations result in thinning, fragility, wrinkles, laxity, impaired wound healing, and a microenvironment conducive to cancer. However, the key factors responsible for these changes have not been fully elucidated and relevant models for the study of skin aging progression are lacking. CCN1, a secreted extracellular matrix (ECM) associated matricellular protein, is elevated in dermal fibroblasts in aged human skin. Towards constructing a mouse model to study key factors involved in skin aging progression, we demonstrate that transgenic mice, with selective expression of CCN1 in dermal fibroblasts (*COL1A2-CCN1*), display accelerated skin dermal aging. The aged phenotype in *COL1A2-CCN1* mice resembles aged human dermis: the skin is wrinkled, and the dermis is thin and composed of loose, disorganized, and fragmented collagen fibrils. These dermal alterations reflect reduced production of collagen due to impaired TGF-β signaling and increased expression of matrix metalloproteinases, driven up induction of c-Jun/AP-1. Importantly, similar mechanisms drive human dermal aging. Taken together, the data demonstrate that elevated expression of CCN1 by dermal fibroblasts functions as a key mediator of dermal aging. The *COL1A2-CCN1* mouse model provides a novel tool for understanding and studying mechanisms of skin aging and age-related skin disorders.

## INTRODUCTION

As the average expected lifespan increases, the consequences of aging are becoming an increasingly prominent public health issue. Aging affects all individuals and is the highest risk factor for most human diseases (Kennedy *et al.*, 2014), including skin diseases (Beauregard and Gilchrest, 1987). Histological and ultrastructural studies of aged skin have revealed prominent alterations in the collagen-rich dermal extracellular matrix (ECM), which comprises the bulk of skin (Jacob, 2003; Yaar and Gilchrest, 2001). These deleterious alterations include loss of dermal mass, due to reduced production (Quan *et al.*, 2010b) and increased fragmentation (Fisher *et al.*, 2009) of dermal collagen fibrils.

Collagen fibrils are responsible for the structural and mechanical support provided by the dermis. Collagen fibrils also serve as a substrate for cellular attachment, which critically regulates cell function (Plant *et al.*, 2009; Sweeney *et al.*, 2008). In addition, the dermal ECM serves as a repository for a variety of bioactive proteins. Therefore, age-related degeneration of dermal collagen fibrils broadly impacts skin function (Smith *et al.*, 1962). Age-related alterations of collagen fibrils also create a tissue microenvironment that is directly related to age-related skin pathologies, such as increased fragility (Ma *et al.*, 2001), impaired vasculature support (Jacob, 2003), poor wound healing (Eaglstein, 1989), and promotion of skin cancer (Rogers *et al.*, 2015).

We previously reported that the matricellular protein CCN1 is markedly elevated in aged human skin (Quan *et al.*, 2006). CCN1 is the first member of the CCN protein family, which comprises six members, CCN1 to CCN6 (Ayer-Lelievre *et al.*, 2001). Members of the CCN family exhibit diverse cellular functions, including regulation of cell proliferation, chemotaxis, apoptosis, adhesion, motility, ion transport, and ECM regulation (Jun and Lau, 2011). CCN1 has been reported to regulate cell adhesion, migration, chemotaxis, inflammation, cell-matrix interactions,

synthesis of ECM proteins, and wound healing (Lau, 2011). CCN1 functions by interacting with multiple integrins in a cell-type and context-dependent manner.

We have previously reported that CCN1 regulates collagen homeostasis through αVβ3 integrin in human skin fibroblasts (Qin *et al.*, 2013). It has been reported that heparin sulfate proteoglycans (HSPGs) bind to CCN1 any may serve as co-receptors (Chen *et al.*, 2000). CCN1 interaction with integrin/HSPGs induces a diverse range of cellular responses including increasing intracellular levels of reactive oxygen species (ROS) (Chen *et al.*, 2007). Chen et al. (EMBO, 2007) demonstrated that exogenously added CCN1 raises ROS levels via ROS generation and release from mitochondria, a phenomenon that is known to contribute to an oxidative stress response. In adult human dermal fibroblasts, ROS negatively regulates collagen production (He *et al.*, 2014), while in fibrogenic myofibroblasts ROS is involved in the stimulation of collagen production (Dosoki *et al.*, 2017; Wermuth *et al.*, 2019). Thus, it appears that the role of ROS in the regulation of collagen production by ROS is complex and dependent on multiple factors, including cell type, the presence of pro-inflammatory mediators, and tissue milieu. Knockout of CCN1 in mice is embryonic lethal. This lethality is primarily due to the impairment of ECM homeostasis which leads to failure of vascular development (Mo *et al.*, 2002).

CCN1 is expressed predominantly in dermal fibroblasts in human skin (Quan *et al.*, 2006), the major cells responsible for collagen homeostasis. Elevated expression of CCN1 in cultured primary adult human dermal fibroblasts causes alterations in the expression of ECM genes similar to those observed in the dermis of aged human skin (Quan *et al.*, 2006).

To explore the role of CCN1 in skin aging we created a transgenic mouse model that selectively expresses CCN1 in dermal fibroblasts using the collagen1A2 (*COL1A2)* enhancer and promoter

sequences. *COL1A2-CCN1* mice exhibit accelerated aging of the dermis, characterized by loss of and fragmentation of collagen fibrils, which closely resembles aged human skin. Mechanistic investigations revealed that CCN1-associated impairment of TGF-β signaling, the major regulator of collagen and other ECM components, contributes to dermal thinning through reduced production of collagen. Furthermore, the upregulation of the transcription factor c-Jun/AP-1 contributes to collagen fibril fragmentation, through elevated expression of multiple matrix metalloproteinases (MMPs), in *COL1A2-CCN1* mice. Thus, fibroblast-derived CCN1 expression orchestrates key age-related changes in dermal ECM by dysregulating both production and homeostasis of collagen.

## RESULTS AND DISCUSSION

### Fibroblast expression of CCN1 induces age-related alterations in the dermal extracellular matrix

*COL1A2-CCN1* mice were generated using a DNA construct containing the protein-coding sequences of human CCN1 under the control of the regulatory sequences of the human COL1A2 proximal gene promoter and upstream enhancer (Figure 1a), which is selectively expressed in fibroblasts (Bou-Gharios *et al.*, 1996; Sonnylal *et al.*, 2010). PCR-based genotyping identified nine *COL1A2-CCN1* transgenic founders, and extensive CCN1 transgene expression was observed throughout the dermis as shown by immunohistology (Figure S1a), quantitative RT-PCR (Figure S1b) and Western blot (Figure S1c). Three lines with similar CCN1 transgene expression in the skin (Figure S1C) were used for the studies presented in this report.

Newborn *COL1A2-CCN1* mice were grossly normal in appearance, and histological evaluation revealed normal skin morphology (Figure S1A). However, by six months of age, all three lines of *COL1A2-CCN1* mice exhibited an aged appearance, characterized by reduced size (Figure 1b)

reduced weight (Figure 1c, 20% less weight compared to control littermates), and wrinkles on their dorsal skin (Figure S2a). The development of the aged appearance began at approximately two months of age and gradually became more apparent during the following four months. The degree of the aged appearance paralleled the accumulation/increases of CCN1 protein in the skin (Figure 1d).

Histological examination revealed dermal thinning in *COL1A2-CCN1* mice by six months of age. Dermal thickness was reduced by 46%, compared to non-transgenic sex and age-matched littermates (Figure 1e). Masson's trichrome (Figure 1f) and Sirius red (Figure S2b) staining, which visualize collagen fibrils, revealed reduced density of collagen fibrils in *COL1A2-CCN1* mice. Nanoscale analysis by atomic force microscopy (AFM) indicated that collagen fibrils were significantly fragmented and disorganized in *COL1A2-CCN1* transgenic mice (Figure 1g). Collagen fibrils displayed an amorphous appearance, with loss of distinct longitudinal fibrillar structure and perpendicular striated pattern (referred to as *D*-spacing), which are characteristic topographic features of intact collagen fibrils. These structural alterations of collagen fibrils resemble those overserved in aged human skin (Qin *et al.*, 2014; Quan *et al.*, 2009). Quantitative analysis demonstrated that the average roughness of collagen fibrils, an indicator of collagen fibril organization, was 2.6-fold greater in *COL1A2-CCN1* mice than in non-transgenic littermates (25 nm vs. 66 nm, Figure 1h).

Importantly, the dermal features observed in *COL1A2-CCN1* mice closely resemble alterations that are observed in the dermis of aged human skin, such as aberrant collagen homeostasis (Qin *et al.*, 2013; Qin *et al.*, 2014; Quan *et al.*, 2006). This finding supports the concept that elevated dermal expression of CCN1 is a critical driver of age-related dermal alterations.

**Impaired TGF-β signaling reduces type I collagen and leads to dermal thinning in**

***COL1A2-CCN1* mice**

To examine possible molecular pathways that promote dermal thinning, we cultured dermal fibroblasts from *COL1A2-CCN1* mice and control littermates. We found that fibroblasts from *COL1A2-CCN1* mice express significantly less type I collagen mRNA (Figure 2a) and protein (Figure 2b). These data are consistent with reduced collagen fibril content and dermal thinning in *COL1A2-CCN1* mice.

The TGF-β pathway is the major regulator of dermal ECM production (Quan *et al.*, 2010b). We investigated the potential involvement of TGF-β signaling in reduced expression of type I collagen in *COL1A2-CCN1* mice fibroblasts. We first examined TGF-β-dependent Smad3 phosphorylation, which plays a critical role in type I procollagen gene expression (Lakos *et al.*, 2004). Interestingly, TGF-β-dependent Smad3 phosphorylation was significantly lower in dermal fibroblasts from *COL1A2-CCN1* mice (Figure 2c). To elucidate the mechanism of impaired TGF-β signaling, we determined the gene expression of the major TGF-β pathway components, including TGF-β ligands, TGF-β receptors, and Smads. We found that levels of type II TGF-β receptor (TβRII) mRNA (Figure 2d) and protein (Figure 2e) were selectively and significantly decreased by 57% and 70%, respectively, in *COL1A2-CCN1* mice fibroblasts. In contrast, type I TGF-β receptor (TβRI) expression (Figures 2d and 2e) and expression of other TGF-β pathway components remained unchanged (Figure S3). Next, we tested the possibility that prevention of TβRII reduction should counteract impaired TGF-β signaling and thereby prevents downregulation of type I collagen. We found that restoration of impaired TGF-β/Smad signaling by infecting *COL1A2-CCN1* fibroblasts with TβRII-expressing adenovirus partially reversed the downregulation of type I collagen mRNA (Figures 2f) and protein (Figure 2g) expression.

These data support the conclusion that specific down-regulation of TβRII impairs TGF-β/Smad

signaling, which leads to a reduction of type I collagen in *COL1A2-CCN1* mice fibroblasts. Consistent with this finding, we previously reported that TGF-β signaling is decreased in aged human skin, largely due to a reduction in TβRII (Fisher *et al.*, 2016; Quan *et al.*, 2006). Given that the TGF-β pathway is the major regulator of collagen production, it is likely that reduced collagen production and attendant dermal thinning in *COL1A2-CCN1* mice is mediated, at least in part, by impaired TGF-β signaling in dermal fibroblasts.

Impairment of TGF-β signaling, due to loss of TβRII in stromal fibroblasts, results in epithelial tumors in animal models (Achyut *et al.*, 2013). In the case of skin cancer, ultraviolet (UV) irradiation from the sun is thought to be the major risk factor. As it relates to this study, UV irradiation simultaneously induces CCN1 (~15-fold) (Quan *et al.*, 2010a) and inhibits expression of TβRII (reduced ~70%) in human skin dermal fibroblasts both *in vivo* and *in vitro* (Quan *et al.*, 2004). These data suggest that a concomitant increase of CCN1 and reduction of TβRII in aged dermal fibroblasts could promote age-related keratinocyte skin cancer, which is the most common cancer in adult Caucasians (Mackiewicz-Wysocka *et al.*, 2013).

**Elevated MMP expression contributes to dermal collagen fibril damage in *COL1A2-CCN1* mice**

We next explored potential mechanisms leading to the fragmentation of collagen fibrils in *COL1A2-CCN1* mice. We measured proteolytic activity, in conditioned media from *COL1A2-CCN1* and non-transgenic littermate fibroblasts, by collagen zymography. As shown in Figure 3a, *COL1A2-CCN1* mice fibroblasts expressed significantly greater proteolytic activity than control fibroblasts. The family of mammalian MMPs is primarily responsible for the degradation of the collagen-rich ECM. Therefore, we examined the ability of the MMP inhibitor GM6001 to suppress proteolytic activity in *COL1A2-CCN1* mice fibroblast conditioned media. GM6001

substantially inhibited *COL1A2-CCN1* mice fibroblast proteolytic activity, in a dose-dependent manner (Figure 3a). This suppression suggests that *COL1A2-CCN1* mice fibroblasts express increased levels of MMPs. To ascertain which MMP family members are expressed by *COL1A2-CCN1* mice fibroblasts, we determined gene expression levels of the 24 mammalian MMPs. We found that expression of MMP-9, -10, -13, -24, and -27 were significantly elevated in fibroblasts from *COL1A2-CCN1* mice compared to control fibroblasts (Figure 3B). Importantly, these changes resemble those in aged human skin, in which elevated CCN1 upregulates expression of MMPs (Qin *et al.*, 2013; Quan *et al.*, 2011).

MMP-13, or collagenase-3, can initiate type I collagen fibril degradation by cleavage at a single site within the triple helix to generate 3/4 and 1/4 length fragments (Stickens *et al.*, 2004). The fragments can be further degraded by MMP-9, also known as gelatinase B (Fanjul-Fernández *et al.*, 2010). MMP-10, or stromelysin-2, degrades other ECM components as well as activates proMMP-13 and proMMP-9 by limited proteolysis (Nakamura *et al.*, 1998). MMP-24 and -27 are relatively less well characterized. MMP-27 contains a transmembrane domain with a unique C-terminal extension (CTE) that promotes its retention in the endoplasmic reticulum (Cominelli *et al.*, 2014), while MMP-24 is a membrane-type MMP, also known as MT5-MMP, which can activate pro-gelatinase A (proMMP-2) in tumors (Llano *et al.*, 1999). Therefore, *COL1A2-CCN1* fibroblasts express elevated levels of MMPs that together can initiate and further degrade type I collagen fibrils.

We next cultured *COL1A2-CCN1* and control littermate fibroblasts in three-dimensional collagen lattices and examined collagen fibril fragmentation by AFM. AFM images revealed that collagen fibrils in lattices containing control fibroblasts were intact and well-organized, displaying characteristic periodic D-banding (Figure 3c, left panel). In contrast, collagen fibrils in lattices containing *COL1A2-CCN1* mice fibroblasts were fragmented and disorganized (Figure 3c,

middle left), similar to collagen fibrils in lattices treated with recombinant human MMP-1 (Figure 3c, right panel). *COL1A2-CCN1* mice fibroblast-mediated collagen fibril disruption was blocked by GM6001 (Figure 3c, middle right).

AFM three-dimensional surface topography mapping indicated that collagen fibrils in lattices containing *COL1A2-CCN1* mice fibroblasts were more disorganized (Figure 3d). Quantitative analysis of AFM data indicated that the average roughness (a measure of fibril organization) of collagen fibrils in lattices containing *COL1A2-CCN1* mice fibroblasts was 2-fold greater than lattices containing control fibroblasts (66 nm vs. 127 nm).

**c-Jun/AP-1 contributes to dermal collagen damage in *COL1A2-CCN1* mice through elevation of MMPs**

Three of the five MMPs that are elevated in *COL1A2-CCN1* mice fibroblasts (MMP-9, -10 and -13) are regulated by the transcription factor AP-1 (Benbow and Brinckerhoff, 1997). We determined the expression of c-Jun, a component of AP-1, and found significant increases in c-Jun mRNA (Figure 4a) and protein (Figure 4b). In addition, AP-1 transcriptional activity, measured by a luciferase reporter, was elevated four-fold in *COL1A2-CCN1* mice fibroblasts (Figure 4c). Importantly, we found that knockdown of c-Jun by two different c-Jun siRNAs (Figure S4) partially reversed the upregulation of multiple MMPs (Figure 4d). We have previously reported that multiple MMPs increase with age in the human dermis (Fisher *et al.*, 2009; Quan *et al.*, 2009), and this increase is associated with elevated expression of c-Jun/AP-1 (Qin *et al.*, 2014). Taken together, these data indicate that CCN1 induction of MMPs likely involves the upregulation of c-Jun/AP-1.

Our data demonstrate that CCN1 is specifically expressed in dermal fibroblasts in mouse skin. The major histological alterations of the epidermis in aged human skin are flattening of the rete

ridges and thinning of the epidermis. We did not observe significant histological epidermal alterations in our *COL1A2-CCN1* mice, although normal mouse epidermis is relatively thin and generally lacks distinct rete ridges, making changes in these features difficult to access. Human aging also results in graying and thinning of hair. We have not observed a hair phenotype in our *COL1A2-CCN1* mice. As such, *COL1A2-CCN1* mice are primarily a model of accelerated dermal aging.

It is possible that the COL1A2-CCN1 cassette that drives CCN1 expression in dermal fibroblasts may express CCN1 in collagen-producing cells in tissues other than skin. To investigate the potential effects of CCN1 transgene expression in tissues other than skin, we performed detailed necropsy of all organs. Histopathological examination did not reveal significant alterations in connective tissues or other tissues (brain, lungs, heart, liver, kidneys, skeletal muscle, joint, bone, tendon, etc.) that distinguished wild-type control littermates from *COL1A2-CCN1* mice (Table S1).

In summary, we demonstrate that selective expression of CCN1 in dermal fibroblasts drives an accelerated aged phenotype in the dermis that closely resembles human aging (Figure 4e). This finding supports a causal link between CCN1 and skin dermal aging. The mechanism by which CCN1 acts is indirect, likely initiated by integrin outside in signaling (Chen *et al.*, 2007) leading to MAP kinase pathway activation and biosynthesis of effectors (Chen *et al.*, 2001) such as AP-1. The COL1A2-*CCN1* mouse model provides a unique opportunity to identify and investigate initial molecular mechanisms and early markers of skin dermal aging. Such studies could lead to the development of novel preventative and ameliorative therapeutic strategies to improve skin health and reduce age-related maladies in the elderly.

## MATERIALS AND METHODS

### Generation of *COL1A2-CCN1* transgenic mice

The *COL1A2-CCN1* transgenic mice used in this study were produced by standard pronuclear injection of linear DNA into a fertilized mouse egg (C57BL/6, Jackson Labs) at the University of Michigan Transgenic Core. Briefly, a Sal1 fragment containing the human CCN1 was PCR amplified and cloned in the plasmid pCD3 containing the 6-kb enhancer and promoter of the COL1A2 gene, an IRES-lacZ reporter, and the murine protamine polyA signal (Bou-Gharios *et al.*, 1996; Sonnylal *et al.*, 2010). All cloning was verified by sequencing. Integration of the CCN1 transgene was assessed by genotyping of mouse tail DNA with specific primers for CCN1 transgene (5'-AAC-CCT-GAG-TGC-CGC-CTT-GTG-AAA-3' and 5'-ATT-GGC-ATG-CGG-GCA-GTT-GTA-GTT-3') and mouse β-globin (5'-CCA-ATC-TGC-TCA-CAC-AGG-ATA-GAG-AGG-GCA-GG-3' and 5'-CCT-TGA-GGC-TGT-CCA-AGT-GAT-TCA-GGC-CAT-CG 3') as a positive control. The *COL1A2-CCN1* founders were crossed with C57BL/6 background breeders (Jackson Labs) for at least 6 generations. All experiments were performed in 6 months-old sex-matched mice. Three lines with similar expression of CCN1 transgene (Figure S1c) were used for the studies presented in this report. All protocols for mouse experimentation were approved by the University of Michigan Institutional Animal Care and Use Committee.

### Histology and Immunohistology

Mouse skin was embedded in OCT and cryo-sections (7μm) were stained with hematoxylin and eosin (H&E), Masson's trichrome, or Sirius red by the standard procedures. The dermal thickness and collagen density (blue in Masson's trichrome and red in Sirius red) were quantified by computerized image analysis (Image-pro Plus software, version 4.1, Media Cybernetics). Immunohistology was performed as described previously using antibodies against CCN1 (Santa

Cruz Biotechnology, Santa Cruz, CA) (Quan *et al.*, 2006), type I procollagen (EMD Millipore, Temecula, CA). Briefly, skin samples embedded in OCT were sectioned (7 µm), fixed in 2% paraformaldehyde, permeabilized with 0.5% Triton X-100 in phosphate-buffered saline (PBS), blocked with rabbit serum (5% in PBS) and incubated for one hour at room temperature with primary antibodies, followed by incubation with secondary antibody for one hour at room temperature. After staining, the slides were examined using a digital imaging microscope (Zeiss, Germany). The specificity of staining was determined by substituting isotype-control immunoglobulin (mouse IgG2a) for the primary antibodies. No detectable staining was observed with isotype-controls.

**Atomic force microscopy (AFM) imaging**

Mouse skin biopsies and three-dimensional collagen lattices were embedded in OCT and cryo-sections (15µm) were mounted on microscope cover glass (1.2 mm diameter, Fisher Scientific Co., Pittsburgh, PA) for AFM image analysis. AFM images were acquired using a Dimension Icon AFM system (Bruker-AXS, Madison, WI) in air using a silicon etched cantilever (NSC15/AIBS, MikroMasch, San Jose, CA) with a full tip cone angle ~40º and the tip radius of curvature ~10 nm. AFM images were acquired at a scan rate of 0.977 Hz, 512x512 pixel resolutions, as previously described (Qin *et al.*, 2014). Collagen fibril's average roughness ($R_a$) was analyzed using Nanoscope Analysis software (Nanoscope Analysis v120R1sr3, Bruker-AXS). AFM images were obtained from the Electron Microbeam Analysis Laboratory (EMAL), University of Michigan College of Engineering, and analyzed using Nanoscope Analysis software (Bruker-AXS).

**Cell culture, RNA isolation, and quantitative real-time PCR**

Mouse dorsal skin was washed with cold phosphate-buffered saline (PBS) and sterilized with 70% ethanol twice. The skin tissue was placed in an empty 100 mm petri, then dissected and minced with surgical scissors using sterile techniques under the hood. The tissue was placed in a flask and was incubated with 10ml of 0.25% trypsinizing solution (Sigma Chemical Co., St. Louis, MO) and 0.02% ethylene diamine tetraacetate (EDTA, Sigma Chemical Co.) at room temperature for 15 minutes. The trypsinizing solution was replaced with fresh solution (10ml) and incubated for one hour. Isolated cells were collected following brief centrifugation and resuspended in Dulbecco's modified Eagle's minimal essential medium (DMEM; Life Technology Inc., Grand Island, NY) supplemented with 10% fetal bovine serum (FBS; Sigma Chemical Co.), penicillin (100 U/ml), streptomycin (100 μg/ml) in a humidified incubator with 5% $CO_2$ at 37°C. Cells were cultured at sub-confluence and utilized between passages 2 and 4. Total RNA was isolated from mouse skin punch biopsy and dermal fibroblasts using a commercial kit (RNeasy mini kit, Qiagen, Chatsworth, CA) according to the manufacturer's protocol. PCR template was prepared by reverse transcription using Taqman Reverse Transcription kit (Applied Biosystems, Foster City, CA). PCR was performed in duplicate with 2 μl of cDNA for the genes of interest using TaqMan Universal PCR Master Mix kit (Applied Biosystems) and a 7300 sequence detector system (Applied Biosystems). PCR procedures were performed with a robotic workstation (Biomek 2000; Beckman Coulter, Inc., Hialeah, FL) to ensure accuracy and reproducibility. Type I procollagen and MMPs mRNA levels were normalized to the mRNA levels of the housekeeping gene, 36B4 (internal control). Type I procollagen and MMPs primers were purchased from Real-Time Primers (Elkins Park, PA). Human CCN1 primers; sense, 5'-TCAAAGACCTGTGGAACTGGTATC-3', anti-sense primer, 5'-CACAAATCC-GGGTTTCTTTCA-3'.

**Western blot analysis**

Whole-cell proteins were extracted, and equal amounts of protein (~40 μg/lane) were resolved by 6-12% gradient sodium dodecyl sulfate-polyacrylamide (SDS) gel electrophoresis and transferred to polyvinylidene difluoride membranes. Membranes were then blocked with PBST (0.1% Tween 20 in PBS) containing 5% nonfat milk for one hour at room temperature. Primary antibodies were incubated for one hour at room temperature. The following antibodies were used for Western blotting: type I procollagen (EMD Millipore), phospho-Smad3 (Cell Signaling Technology, Danvers, MA), total Smad3, CCN1, TβRI, TβRII, c-Jun (Santa Cruz Biotechnology) and β-actin (Sigma). The membranes were washed three times with PBST solution and incubated with appropriate secondary antibodies for one hour at room temperature. After washing three times with PBST, the membranes were developed with ECF (Vistra ECF Western blotting system, GE Health Care, Piscataway, NJ) following the manufacturer's protocol. The membranes were scanned with a STORM PhosphorImager (Molecular Dynamics, Sunnyvale, CA), the intensities of each band were quantified using ImageQuant software (GE Health Care, Piscataway, NJ) and normalized to β-actin (control). Full-size Western blots are provided in Figure S5.

**Adenovirus infection, siRNA transfection, and AP-1 reporter assay**

TβRII adenovirus was purchased from Applied Biological Materials Inc. (Richmond, BC, Canada). TβRII adenovirus was amplified by transducing HEK293 cells and infected cells following the manufacture's instruction. Control adenovirus was obtained from the University of Michigan Medical School Biomedical Research Core. Control non-silencing si RNA (AATTCTCCGAACGTGTCACGT) and c-Jun si RNA#1 (AAAGTCATGAACCACGTTAA) were purchased from Qiagen (Germantown, MD). c-Jun siRNA #2 (AACTCATGCTAACGCAGCAGT) was purchased from Xeragon Inc (Germantown, MD). AP-1 reporter construct (pAP1-TA-Luc) was purchased from BD Biosciences Clontech (Palo

Alto, CA). Mouse skin fibroblasts were transiently transfected si RNAs or AP-1 reporter construct for 48 hours by electroporation using dermal fibroblasts nucleofector kit (Amaxa Biosystems, Gaithersburg, MD) according to the manufacturer's protocol. Luciferase activity was measured by luciferase assay using an enhanced luciferase assay kit (PharMingen International, San Diego, CA) according to the manufacturer's protocol. Aliquots containing identical β-galactosidase activity were used for each luciferase assay.

**Three-dimensional (3D) collagen cultures and zymography assay**

3D collagen gels were prepared based on a previous publication with minor modifications (Qin *et al.*, 2014). Briefly, rat tail type-I collagen (2 mg/ml, BD Biosciences) was suspended in a medium cocktail (DMEM, NaHCO3 [44 mM], L-glutamine [4 mM], Folic Acid [9 mM]), and neutralized with 1N NaOH to pH 7.2. Cells ($0.5x10^6$) were suspended in 2 ml collagen and medium cocktail solution and plated in a 35 mm bacterial culture dish. The collagen gels were placed in an incubator at 37°C for 30 minutes to allow collagen polymerization. The collagen gels were then incubated with 2 ml media (DMEM, 10% FBS) at $37^0$C, 5% $CO_2$. To activate secreted MMP-1, collagen lattices were washed extensively with PBS (at least three times for 30 minutes) and then treated with Trypsin-EDTA (100 ng/ml, Invitrogen Life Technology, Carlsbad, CA) in serum-free media for 24-36 hours. 3D collagen gels were embedded in OCT and cryo-sections (15 µm) were analyzed for collagen fragmentation by AFM image analysis. For zymography assays, conditioned media from the cultured cells were concentrated and then analyzed by electrophoresis in the presence of 12% Zymogram (collagen) protein gel (Thermal Fisher Scientific, Waltham, MA). After electrophoresis, the gel was incubated in Zymogram Renaturing buffer (Thermal Fisher Scientific) for 30 minutes at room temperature with gentle agitation. After renaturing, the gel was incubated in developing buffer (Thermal Fisher Scientific) at 37°C overnight. The MMPs activities were visualized by staining Coommasie Blue

R-250 (Thermal Fisher Scientific) solution. MMP inhibitor (GM6001, Santa Cruz Biotechnology) was used to test MMP-mediated proteolytic activity.

**Statistical analysis**

Data are expressed as mean ± SEM. Comparisons were made with the unpaired t-test (two groups). ANOVA test was performed for multiple comparisons. All p values are two-tailed and considered significant when <0.05.

**Data availability statement**

The authors confirm that the data supporting findings of this study are available in the article and its Supplementary Materials. There were no data sets used in this study.

**Study approval**

Protocols for mouse experimentation were approved by the University of Michigan Institutional Animal Care and Use Committee.

## CONFLICT OF INTEREST

The authors state no conflict of interest.

## ACKNOWLEDGMENTS

The authors thank Diane Fiolek for administrative assistance, as well as Joel Maust, for writing/editorial support. The authors thank Ingrid Bergin VDM, Pathologist and Director, In Vivo Animal Core, University of Michigan, Unit for Laboratory Animal Medicine for performing mouse necropsy.

Additional thanks to the University of Michigan Transgenic Core for production of *COL1A2-CCN1* mice, and Dr. Shonali Majumdar (University of Texas MD Anderson Cancer Center) for

the pCD3 plasmid containing the 6-kb enhancer and promoter of the Col1a2 gene. This work was supported by the National Institutes of Health (AG054835 to GJF and TQ).

**Author Contributions**

Conceptualization: TQ, JV, GB, GF; Data Curation: TQ, ZQ; Formal Analysis: TQ, GF; Funding Acquisition: TQ, JV, GF; Investigation: YX, YL, ZQ, YY; Methodology: TQ, GF, AD, GB; Project Administration: TQ, GF; Resources: TQ, GB; Supervision: TQ, AD, GF; Validation: TQ, GF; Visualization: TQ, GF, AD, JV; Writing: TQ, GF, AD, GB, JV. All authors read and approved the manuscript.

## REFERENCES

Achyut BR, Bader DA, Robles AI, Wangsa D, Harris CC, Ried T, *et al.* (2013) Inflammation-mediated genetic and epigenetic alterations drive cancer development in the neighboring epithelium upon stromal abrogation of TGF-beta signaling. *PLoS Genet* 9:e1003251.

Ayer-Lelievre C, Brigstock D, Lau L, Pennica D, Perbal B, Yeger H (2001) Report and abstracts on the first international workshop on the CCN family of genes. *Mol Pathol* 54:105-20.

Beauregard S, Gilchrest BA (1987) A survey of skin problems and skin care regimens in the elderly. *Arch Dermatol* 123:1638-43.

Benbow U, Brinckerhoff CE (1997) The AP-1 site and MMP gene regulation: what is all the fuss about? *Matrix Biol* 15:519-26.

Bou-Gharios G, Garrett LA, Rossert J, Niederreither K, Eberspaecher H, Smith C, *et al.* (1996) A potent far-upstream enhancer in the mouse pro alpha 2(I) collagen gene regulates expression of reporter genes in transgenic mice. *J Cell Biol* 134:1333-44.

Chen CC, Mo FE, Lau LF (2001) The angiogenic factor Cyr61 activates a genetic program for wound healing in human skin fibroblasts. *J Biol Chem* 276:47329-37.

Chen CC, Young JL, Monzon RI, Chen N, Todorovic V, Lau LF (2007) Cytotoxicity of TNFalpha is regulated by integrin-mediated matrix signaling. *EMBO J* 26:1257-67.

Chen N, Chen CC, Lau LF (2000) Adhesion of human skin fibroblasts to Cyr61 is mediated through integrin alpha 6beta 1 and cell surface heparan sulfate proteoglycans. *J Biol Chem* 275:24953-61.

Cominelli A, Halbout M, N'Kuli F, Lemoine P, Courtoy PJ, Marbaix E, *et al.* (2014) A unique C-terminal domain allows retention of matrix metalloproteinase-27 in the endoplasmic reticulum. *Traffic (Copenhagen, Denmark)* 15:401-17.

Dosoki H, Stegemann A, Taha M, Schnittler H, Luger TA, Schroder K, *et al.* (2017) Targeting of NADPH oxidase in vitro and in vivo suppresses fibroblast activation and experimental skin fibrosis. *Exp Dermatol* 26:73-81.

Eaglstein WH (1989) Wound healing and aging. *Clin Geriatr Med* 5:183-8.

Fanjul-Fernández M, Folgueras AR, Cabrera S, López-Otín C (2010) Matrix metalloproteinases: Evolution, gene regulation and functional analysis in mouse models. *Biochimica et Biophysica Acta (BBA) - Molecular Cell Research* 1803:3-19.

Fisher GJ, Quan T, Purohit T, Shao Y, Moon KC, He T, *et al.* (2009) Collagen fragmentation promotes oxidative stress and elevates matrix metalloproteinase-1 in fibroblasts in aged human skin. *American Journal of Pathology* 174:101-14.

Fisher GJ, Shao Y, He T, Qin Z, Perry D, Voorhees JJ, *et al.* (2016) Reduction of fibroblast size/mechanical force down-regulates TGF-beta type II receptor: implications for human skin aging. *Aging Cell* 15:67-76.

He T, Quan T, Shao Y, Voorhees JJ, Fisher GJ (2014) Oxidative exposure impairs TGF-beta pathway via reduction of type II receptor and SMAD3 in human skin fibroblasts. *Age (Dordr)* 36:9623.

Jacob MP (2003) Extracellular matrix remodeling and matrix metalloproteinases in the vascular wall during aging and in pathological conditions. *Biomed Pharmacother* 57:195-202.

Jun JI, Lau LF (2011) Taking aim at the extracellular matrix: CCN proteins as emerging therapeutic targets. *Nat Rev Drug Discov* 10:945-63.

Kennedy BK, Berger SL, Brunet A, Campisi J, Cuervo AM, Epel ES, *et al.* (2014) Geroscience: linking aging to chronic disease. *Cell* 159:709-13.

Lakos G, Takagawa S, Chen SJ, Ferreira AM, Han G, Masuda K, *et al.* (2004) Targeted disruption of TGF-beta/Smad3 signaling modulates skin fibrosis in a mouse model of scleroderma. *Am J Pathol* 165:203-17.

Lau LF (2011) CCN1/CYR61: the very model of a modern matricellular protein. *Cell Mol Life Sci* 68:3149-63.

Llano E, Pendas AM, Freije JP, Nakano A, Knauper V, Murphy G, *et al.* (1999) Identification and characterization of human MT5-MMP, a new membrane-bound activator of progelatinase a overexpressed in brain tumors. *Cancer Res* 59:2570-6.

Ma W, Wlaschek M, Tantcheva-Poor I, Schneider LA, Naderi L, Razi-Wolf Z, *et al.* (2001) Chronological ageing and photoageing of the fibroblasts and the dermal connective tissue. *Clin Exp Dermatol* 26:592-9.

Mackiewicz-Wysocka M, Bowszyc-Dmochowska M, Strzelecka-Węklar D, Dańczak-Pazdrowska A, Adamski Z (2013) Basal cell carcinoma - diagnosis. *Contemporary oncology (Poznan, Poland)* 17:337-42.

Mo FE, Muntean AG, Chen CC, Stolz DB, Watkins SC, Lau LF (2002) CYR61 (CCN1) is essential for placental development and vascular integrity. *Mol Cell Biol* 22:8709-20.

Nakamura H, Fujii Y, Ohuchi E, Yamamoto E, Okada Y (1998) Activation of the precursor of human stromelysin 2 and its interactions with other matrix metalloproteinases. *European journal of biochemistry* 253:67-75.

Plant AL, Bhadriraju K, Spurlin TA, Elliott JT (2009) Cell response to matrix mechanics: Focus on collagen. *Biochimica et Biophysica Acta (BBA) - Molecular Cell Research* 1793:893-902.

Qin Z, Fisher GJ, Quan T (2013) Cysteine-rich protein 61 (CCN1) domain-specific stimulation of matrix metalloproteinase-1 expression through alphaVbeta3 integrin in human skin fibroblasts. *J Biol Chem* 288:12386-94.

Qin Z, Okubo T, Voorhees JJ, Fisher GJ, Quan T (2014) Elevated cysteine-rich protein 61 (CCN1) promotes skin aging via upregulation of IL-1beta in chronically sun-exposed human skin. *Age (Dordr)* 36:353-64.

Quan T, He T, Kang S, Voorhees JJ, Fisher GJ (2004) Solar ultraviolet irradiation reduces collagen in photoaged human skin by blocking transforming growth factor-β type II receptor/Smad signaling. *American Journal of Pathology* 165:741-51.

Quan T, He T, Shao Y, Lin L, Kang S, Voorhees JJ, *et al.* (2006) Elevated cysteine-rich 61 mediates aberrant collagen homeostasis in chronologically aged and photoaged human skin. *Am J Pathol* 169:482-90.

Quan T, Qin Z, Robichaud P, Voorhees JJ, Fisher GJ (2011) CCN1 contributes to skin connective tissue aging by inducing age-associated secretory phenotype in human skin dermal fibroblasts. *J Cell Commun Signal* 5:201-7.

Quan T, Qin Z, Xia W, Shao Y, Voorhees JJ, Fisher GJ (2009) Matrix-degrading metalloproteinases in photoaging. *J Investig Dermatol Symp Proc* 14:20-4.

Quan T, Qin Z, Xu Y, He T, Kang S, Voorhees JJ, *et al.* (2010a) Ultraviolet irradiation induces CYR61/CCN1, a mediator of collagen homeostasis, through activation of transcription factor AP-1 in human skin fibroblasts. *J Invest Dermatol* 130:1697-706.

Quan T, Shao Y, He T, Voorhees JJ, Fisher GJ (2010b) Reduced expression of connective tissue growth factor (CTGF/CCN2) mediates collagen loss in chronologically aged human skin. *J Invest Dermatol* 130:415-24.

Rogers HW, Weinstock MA, Feldman SR, Coldiron BM (2015) Incidence Estimate of Nonmelanoma Skin Cancer (Keratinocyte Carcinomas) in the US Population, 2012. *JAMA Dermatol* 151:1081-6.

Smith JG, Jr., Davidson EA, Sams WM, Jr., Clark RD (1962) Alterations in human dermal connective tissue with age and chronic sun damage. *J Invest Dermatol* 39:347-50.

Sonnylal S, Shi-Wen X, Leoni P, Naff K, Van Pelt CS, Nakamura H, *et al.* (2010) Selective expression of connective tissue growth factor in fibroblasts in vivo promotes systemic tissue fibrosis. *Arthritis Rheum* 62:1523-32.

Stickens D, Behonick DJ, Ortega N, Heyer B, Hartenstein B, Yu Y, *et al.* (2004) Altered endochondral bone development in matrix metalloproteinase 13-deficient mice. *Development* 131:5883-95.

Sweeney SM, Orgel JP, Fertala A, McAuliffe JD, Turner KR, Di Lullo GA, *et al.* (2008) Candidate cell and matrix interaction domains on the collagen fibril, the predominant protein of vertebrates. *J Biol Chem* 283:21187-97.

Wermuth PJ, Mendoza FA, Jimenez SA (2019) Abrogation of transforming growth factor-beta-induced tissue fibrosis in mice with a global genetic deletion of Nox4. *Lab Invest* 99:470-82.

Yaar M, Gilchrest BA (2001) Skin aging: postulated mechanisms and consequent changes in structure and function. *Clin Geriatr Med* 17:617-30, v.

## FIGURE LEGENDS

**Figure 1. Transgene expression of CCN1 in dermal fibroblasts causes age-related alterations of the dermal aged phenotype in mouse skin dermis.** (**a**) Schematic representation of the construct expressed in dermal fibroblasts. (**b**) Representative gross appearance of 6 months old COL1A2-CCN1 mouse (right) and their non-transgenic littermate control (CTRL) (left). (**c**) Bodyweight of *COL1A2-CCN1* mice and their non-transgenic littermate control (CTRL) was measured at 6 months after birth ($n$=6 mice per genotype). (**d**) Accumulation of CCN1 protein expression in *COL1A2-CCN1* mice and their non-transgenic littermate control (CTRL) over six months. Inset shows representative Western blots. CCN1 protein relative levels were determined by quantification of band intensity after normalization to the internal control β-actin band intensity. (**e**) H&E staining in samples taken from non-transgenic littermate control (CTRL) and *COL1A2-CCN1* mice, with representative images shown. The dermal thickness was quantified by computerized image analysis (Image-pro Plus software, version 4.1, Media Cybernetics, Rockville, MD). (**f**) Masson's trichrome staining, representative images. The dermal collagenous extracellular matrix is stained blue, cells are stained red, and the nuclei black. Subcutaneous fat appears white. Collagen fibril staining (blue) per microscopic field was quantified by ImageJ software. (**g**) Atomic force microscopy of collagen fibrils. Scale bar = 200 nm. Representative images are shown. The blue arrowheads indicate intact collagen fibrils and red arrowheads indicate damaged collagen fibrils. (**h**) Dermal collagen fibril organization, measured as Collagen fibril average roughness ($R_a$, nm), was quantified using Nanoscope Analysis software (Nanoscope_Analysis_v120R1sr3, Bruker-AXS, Santa Barbara, CA). All results expressed as mean ± SEM, $n$=3 mice per genotype, *$p < 0.05$. Scale bars = 100 µm (e-f), 200 µm (g).

**Figure 2. Reduced production of type I collagen and impaired TGF-β signaling in fibroblasts from *COL1A2-CCN1* mice.** Fibroblasts from six months old *COL1A2-CCN1* mice and non-transgenic littermate control (CTRL) were cultured from dorsal skin. Fibroblasts from *COL1A2-CCN1* and CTRL mice were analyzed for levels of (**a**) type I procollagen mRNA, (**b**) type I procollagen protein, (**c**) TGF-β induction of Smad3 phosphorylation, (**d**) type I (TβRI) and type II (TβRII) TGF-β receptor mRNA, and (**e**) TβRI and TβRII protein. mRNA and protein levels determined by real-time RT-PCR or Western analysis, respectively. mRNA or protein levels were normalized to 36B4 (internal housekeeping gene control) or β-actin (loading control), respectively. Inset shows representative Western blots. Restoration of impaired TGF-β/Smad signaling by infecting *COL1A2-CCN1* fibroblasts with TβRII-expressing adenovirus partially reversed the downregulation of type I collagen mRNA (**f**) and protein (**g**) expression. Mean ± SEM, $n=3$ mice per genotype, *$p < 0.05$.

**Figure 3. Fibroblasts from *COL1A2-CCN1* mice express elevated levels of collagen-degrading matrix metalloproteinases (MMPs).** (**A** and **B**) Fibroblasts from the dorsal skin of six months old *COL1A2-CCN1* mice and non-transgenic littermate control (CTRL) were cultured in monolayer. (**a**) Proteolytic activities in fibroblast conditioned media were examined by zymography. Areas of protease activity appear as clear bands. Inhibition of proteolytic activity by MMP inhibitor GM6001 identified the presence of MMP proteolytic activity. Recombinant human matrix metalloproteinase 1 (rh-MMP-1) was used as a positive control. (**b**) MMP mRNA levels were determined by real-time RT-PCR. Levels were normalized to 36B4 (internal housekeeping gene control). (**c** and **d**) Fibroblasts from *COL1A2-CCN1* and non-transgenic littermates (CTRL) were cultured in three-dimensional collagen lattices and the structure of the collagen fibrils was examined by atomic force microscopy (AFM) in different treatment conditions. (**c**) The red arrows indicate intact collagen fibrils and blue arrowheads indicate

damaged collagen fibrils. (**d**) Collagen fibril organization, measured by average roughness ($R_a$), was quantified using Nanoscope Analysis software (Nanoscope_Analysis_v120R1sr3, Bruker-AXS, Santa Barbara, CA). All data expressed as mean ± SEM, $n=3$ mice per genotype, *p < 0.05.

**Figure 4. c-Jun/AP-1 contributes to dermal damage in *COL1A2-CCN1* mice through elevation of MMPs.** Fibroblasts from dorsal skin of six months old non-transgenic littermate control (CTRL) and *COL1A2-CCN1* mice were cultured in monolayer. (**a**) c-Jun mRNA and (**b**) c-Jun protein levels were determined by real-time RT-PCR and Western analysis, respectively. Levels were normalized to 36B4 (internal housekeeping gene control) and β-actin (loading control). Inset shows representative Western blots. (**c**) An AP-1 reporter construct (pAP1-TA-Luc) was transiently transfected by electroporation into control and *COL1A2-CCN1* fibroblasts. After 48 hours, luciferase activity was measured to determine AP-1 activity. (**d**) Knockdown of c-Jun by c-Jun siRNA partially reversed upregulation of multiple MMPs. Fibroblasts from six month old COL1A2-CCN1 mice were transiently transfected with control siRNA (CTRL) or c-Jun siRNA #1 or #2 by electroporation. Cells were harvested 48 hours after transfection and analyzed for MMP mRNA levels by real-time RT-PCR. Levels normalized to 36B4 (internal housekeeping gene control). mean ± SEM, n=3, *p < 0.05 vs CTRL. (**e**) Model showing mechanisms by which elevated CCN1 leads to dermal ECM aging. All data expressed as mean ± SEM, $n=3$ mice per genotype, *p < 0.05 vs CTRL.

Figure 1

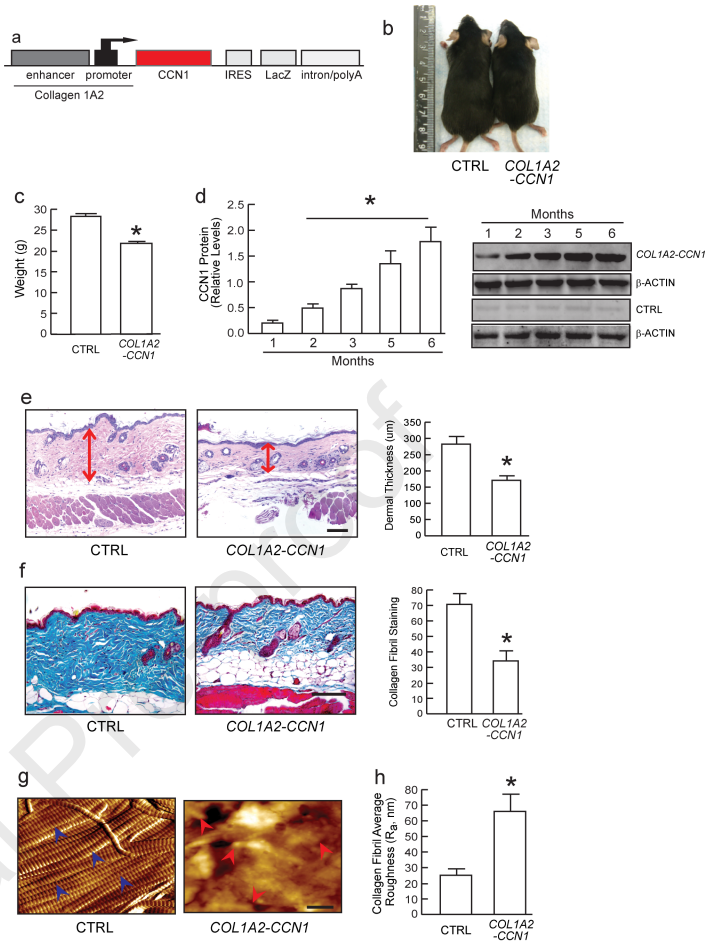

Figure 2

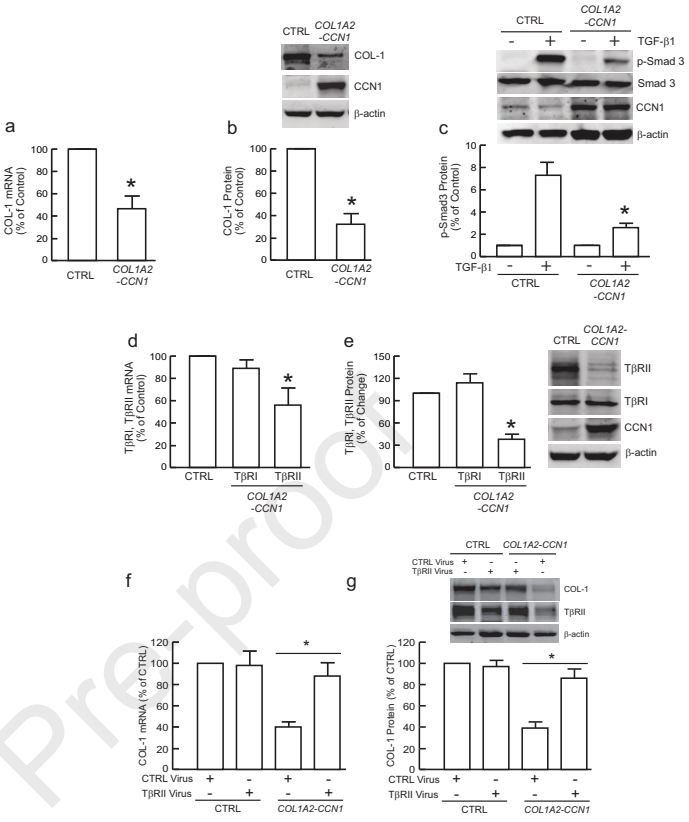

Figure 3

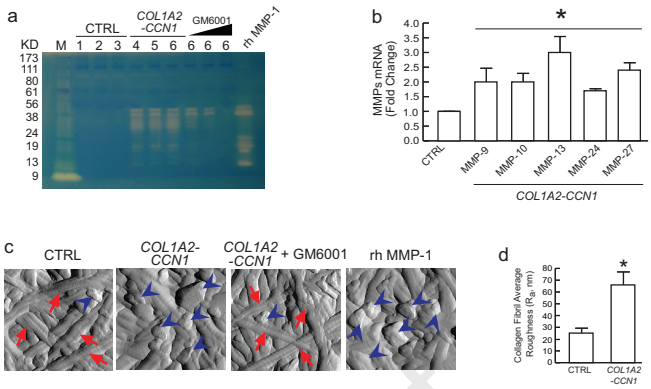

Figure 4